Proceedings of ASME Turbo Expo 2011
GT2011
June 6-10, 2011, Vancouver, British Columbia, Canada

GT2011-45943

MODEL-BASED DATA RECONCILIATION AND BIAS DETECTION FOR HEAVY-DUTY INDUSTRIAL GAS TURBINES PERFORMANCE DIAGNOSIS

TsungPo Lin
Service Engineering
GE Energy
Atlanta, GA 30339

Eduardo Mendoza
Service Engineering
GE Energy
Atlanta, GA 30339

Brian K. Kestner
Aerospace Systems Design Laboratory
School of Aerospace Engineering
Georgia Institute of Technology
Atlanta, GA 30332

ABSTRACT

Performance diagnoses of heavy-duty industrial gas turbines often rely on measured data from on-site monitoring systems (OSM), subjected to larger uncertainties and possible biases. The measured data are used to analyze gas turbine heat balance and estimate immeasurable performance characteristics such as firing temperature and component health parameters. Traditional heat balance techniques are deterministic, and, thus, calibration uncertainty is not mitigated. In this paper, a method of model-based data reconciliation (MBDR) and bias detection was developed, serving as a probabilistic process of reducing calibration uncertainty while eliminating contamination effects caused by measurement biases. This method utilizes physics-based gas turbine models to reconcile multiple data sets while the model health parameters are inferred simultaneously. Levenberg–Marquardt algorithm was utilized to solve the maximum-likelihood problem, i.e., minimizing Least Squares. A hypothesis test scheme using sequential bias compensation was utilized for bias detection and neutralizing smearing effects. To reduce the computation time in MBDR and bias detection, the Response Surface Methodology (RSM) was applied to generate surrogate model. A systematic way of data selection using Multiscale Principal Component Analysis was also employed, serving as an efficient way of filtering large data sets for the use of MBDR. This proposed methodology was demonstrated by application to GE 7FA gas turbines. Results showed significant reduction in calibration uncertainty and smearing effects.

INTRODUCTION

Continuous monitoring gas turbine performance through the on-site monitoring system (OSM) has been widely adopted by the power plant industry since it provides the real-time information for better understanding the current machine status. This is especially important for the OEM companies, such as GE, who need to propose the upgrade package and provide absolute performance guarantees based on the current degradation status. There has been, however, a lack of a systematic methodology for analyzing the OSM data and tackling the problem of measurement uncertainty and bias. The measurement errors cause major issues in gas turbine performance analyses, such as not able to represent true status of the machine and, thus, force the analyzer to impose more margins on the performance guarantees to reduce the risks. Traditional data matching, or "data reduction", is a deterministic method not capable of mitigating the estimate errors due to measurement uncertainty.

Data reconciliation is a technique developed to reduce the effect of random errors and improve the measurement accuracies. It utilizes process model constraints and estimates process variables by adjusting the measurements so that the estimates satisfy the model constraints. The reconciled true value estimates are expected to be more accurate than the measurements and, most importantly, satisfy the physical constraints such as conservation of energy and mass.

Data reconciliation has been widely implemented in the chemical industries during the past 35 years. There is a large volume of literature available addressing related topics. A detailed description of the underlying concepts and application examples can be found in Romagnoli and Sanchez [1]. Data reconciliation for linear models is also well studied. Crowe et al. [2] used a matrix projection method to decompose the model constraints and solve for the measured and unmeasured parameters sequentially. Pai and Fisher [3] use Crowe's matrix projection method to decompose the linearized sub-problems and Broyden's method to update the Jacobian. Swartz [4] also uses Crowe's method along with a QR matrix factorization to eliminate the unmeasured parameters.

The presence of biases can contaminate the results of data reconciliation. A bias is statistically an error whose occurrence as the result of a random variable is highly unlikely. The presence of a measurement bias is usually detected by statistical tests generally based on linear or nonlinear models. Rejection of biases can be performed using confidence level or values when the underlying distribution function for the measurement is available. Many works of bias detection have been done in chemical industry and can be found in [5-8]. Most works on data reconciliation and bias detection were mainly from chemical industry. These techniques were best suited for solving the

*QR matrix: Q - orthogonal matrix; R - upper triangular matrix bilinear conservation equations such as mass and energy balance with one data set, and, as a result, might not be suited for gas turbine model calibration problems, which often processes large amount of OSM data.

Application of data reconciliation in the power generation industry is not as widespread as in the chemical industry. However, there have been significant contributions: An equation-based data validation technique proposed by Cheng et al. was implemented to the gas turbine performance monitoring system [9]. Hartner et al. [10] suggested a model-based data reconciliation method and applied it to a fossil boiler plant. Gulen and Smith [11] developed analytical solutions to the data reconciliation problem based on the concept of the Kalman filter. Theses works, however, mainly focused on solving the reconciliation problems considering uncertainty only, while the issues of measurement biases were not addressed.

Inference of jet engine health parameters from measurement data is often defined as gas path analysis (GPA). A large number of research works showing different GPA approaches including linear and non-linear GPA [12-14] were for specific engine types and might not be adapted to other types of applications with different prior assumption about the engine configuration. Applying one of these techniques to a different engine configuration could lead to contaminated results due to smearing effects not caused by measurement biases but by the model itself.

Based on challenges in gas turbine performance analyses and previous research works done in this field, developing a methodology capable of processing multiple OSM data sets and performing probabilistic model calibration with the consideration of measurement bias is necessary.

NOMENCLATURE

AFPAP	=	Barometric Pressure
AFPCS	=	Compressor Inlet Pressure Drop
AFPEP	=	Exhaust Pressure Drop
AFQ	=	Compressor Airflow
CHUM	=	Ambient Humidity
CTIM	=	Compressor Inlet Temperature
CPD	=	Compressor Discharge Pressure
CTD	=	Compressor Discharge Temperature
CPR	=	Compressor Pressure Ratio
CQ	=	Stage 1 Nozzle Inlet Flow Function
DMM	=	Data Matching Multipler
DPF	=	Power Factor
DWATT	=	Generator Output
FQG	=	Fuel Flow
FTG	=	Fuel Temperature
HTC	=	Heat Transfer Correction Factor
IGV	=	Inlet Guide Vane
PDF	=	Probability Density Function
Tfire	=	Firing Temperature
THN	=	Compressor Rotation Speed
TTXM	=	Turbine Exhaust temperature
comp	=	Compressor
comb	=	Combustor
eff	=	Efficiency
turb	=	Turbine

METHODOLOGY

The methodology proposed here is trying to resolve the following challenges in gas turbine performance analyses:

- Reconcile multiple data sets while calibrating the model
- Mitigate smearing effects caused by measurement biases
- Filter large OSM data sets used for model calibration
- Reduce the computation time

The goal is to provide a framework of probabilistic model calibration with multiple data sets, considering measurement uncertainties and biases. Model-based data reconciliation (MBDR) is the core part of this methodology.

Model-Based Data Reconciliation

Model-based data reconciliation (MBDR) utilizes the physics-based model to reconcile the data. MBDR is mathematically an inference process where model parameters are inferred from the source data through an optimization process. The source data are either the raw measured data or preprocessed data, e.g., filtered data, denoised data, etc. The parameters to be inferred are often the performance correction factors (tuners or multipliers), which “tune” the system off-design performance to be consistent with test results. In MBDR, model calibration and data reconciliation are carried out simultaneously, where the source data are reconciled by inferring the model tuners while the model tuners are calibrated by reconciled data. It is recognized that when a plant model such as a GTP cycle deck, a gas turbine performance simulation tool by GE, or a GateCycle™ model, a combined cycle performance simulation tool by GE, is used for performance simulation, any set of performance metrics that are generated by the system model, e.g., flow/pressure/temperature of gas/water/steam, is ensured to be thermodynamically consistent, and, therefore, automatically becomes a set of candidate solutions for data reconciliation. It is also known that these model-predicted performance metrics are functions of the model inputs such as ambient conditions, operation parameters, system configuration, and system degradations, which are mimicked by a set of performance correction factors, e.g., DMM’s (Data Match Multipliers) in GTP cycle deck and similar factors in other performance models. Combining the above two facts, if these model-predicted metrics are also measured with uncertainties, one can perform data reconciliation in such a way that the Least Squares objective function, which is defined by the differences between the model-predicted and measured values for the performance metrics, is minimized by an optimum set of model inputs. This is the core concept of Least Squares MBDR, and can be expressed as follows:

$$\min_{\theta_j} \sum_{i=1}^{N} \left(\frac{y'_i - f(\theta_j)}{\sigma_i} \right)^2 \quad (1)$$

where y'_i are the given measurements; $f(\theta_j)$ are the unknown reconciled values, which are functions of unknown model input variables, θ_j, to be solved for; σ_i represents the measurement uncertainties.

Identifying appropriate model inputs and outputs are crucial for MBDR. Typical model inputs include ambient conditions, operation parameters, system configurations, and degradation effects. One should limit the number of model inputs related to ambient and operation parameters to maintain enough redundancy, while remaining all health parameters, which represent system degradation status. Table 1 lists the gas turbine model inputs and outputs used in this study.

Table 1 Gas turbine model parameters in MBDR

Model Outputs (To be reconciled)	**Model Inputs** (Fixed)	**Calibration Factors** (To be estimated)
DWATT	CTIM	comp_flow_DMM
FQG	AFPAP	comp_eff_DMM
AFQ	CHUM	comb_eff_DMM
CPD	AFPCS	turb_eff_DMM
CTD	AFPEP	turb_CQ_DMM
TTXM	IGV	Tfire
	DPF	
	FTG	
	THN	

Eq. 1 is solved by the nonlinear solver. Several Nonlinear Programming (NLP) techniques such as Conjugate Gradient, Gaussian Newton, and Sequential Quadratic Programming (SQP) were investigated. It was found as the solutions were far away from their initial values, i.e., significant performance degradation from its new and clean status, these techniques did not show good convergence features, i.e., the value of Least Squares objective function equals zero when MBDR is in the data matching mode. On the other hand, the Levenberg-Marquardt algorithm demonstrated a good convergence capability in a wide range of degradation status and simulated bias scenarios [15], and, therefore, was selected as the nonlinear solver for MBDR.

Levenberg-Marquardt (LM) algorithm [16] is a nonlinear optimization technique most suitable for solving the type of objective function expressed as the sum of squares of a nonlinear function. The LM algorithm can be thought of as a combination of steepest descent and Gauss-Newton expansion methods. It significantly outperforms gradient descent and conjugate gradient methods in a wide range of problems as well. LM is a pseudo-second order method that uses the sum of outer products of the function gradients to estimate the Hessian matrix. Because of its superior performance in solving the least-square type function, the LM algorithm is utilized to solve the nonlinear model based data reconciliation problem in this study.

In solving the MBDR problem, a large number of function calls for the system model is required. The use of Response Surface Methodology (RSM) can save significant computation time. RSM provides a fast-executed model with the analytical polynomial form that spans the entire design space within limited ranges for a complex system response in which no analytical solution exists. RSM includes a number of statistical techniques for creating an empirical relation between an output variable, i.e., response, and the levels of a number of input variables. A typical second-degree response surface equation is given by:

$$R = b_0 + \sum_{i=1}^{n} b_i x_i + \sum_{i=1}^{n}\sum_{j=1}^{n} b_{ij} x_i x_j \tag{2}$$

where b_0 is the intercept term, while b_i, and b_{ij} are the coefficients for the linear terms and the product terms that include the pure quadratic parts b_{ii} and the cross-product parts b_{ij}; x_i are the values for each of the input variables that span the design space and affect the response R directly. In this study the Monte Carlo Simulation is applied to generate random cases for gas turbine model outputs over selected model parameters. The simulated data are then used to obtain the RSE coefficients through nonlinear regression. Number of runs is between 1000 and 2000 to get a good regression model.

Bias Detection

Smearing effects occur when measurement biases exist. In the MBDR application, the smearing effects become more obvious when there is degree of freedom in data reconciliation. When smearing effects happen, the reconciliation process drives the solutions toward the measurements with biases; while, on the other hand, the corrections to “healthy” measurements are beyond the scope of measurement uncertainties, i.e., over-corrections. In this study, the hypothesis testing on different bias models was utilized to form the bias detection scheme. For the MBDR application, the bias model can be expressed as:

$$y' = f(a, \theta) + \varepsilon + b \tag{3}$$

where $f(a, \theta)$ is the system model as a function of the model parameters a, θ, while b is the vector of biases; ε is the vector of random errors. If the measurement data are compensated with the correct gross error model, the compensated data are subject to random errors only, and, therefore, smearing effects will not occur during data reconciliation. The occurrence of smearing effects can be indicated by the test statistics, such as Least Squares. Thus, one can utilize the hypothesis testing to verify the bias model. While applying the hypothesis testing to the bias detection scheme, the null hypothesis and alternative hypothesis can be stated as follows:

H_0: without the bias model there is no smearing effect

$$P(\tau \leq \tau_c \mid \boldsymbol{y_c}' = \boldsymbol{y}') = (1 - \alpha) \tag{4}$$

H_1^g: with the gross error model there is no smearing effect

$$P(\tau \leq \tau_c \mid \boldsymbol{y_c}' = \boldsymbol{y}' - \boldsymbol{b}) = (1 - \alpha) \tag{5}$$

where τ is the test statistics obtained from the result of data reconciliation. By compensating the measured data with a correct gross error model, one can neutralize the smearing effects while carrying out the least squares type data reconciliation. In order to obtain the statistically “correct” bias model, a bias detection technique utilizing hypotheses testing is required. In this study, it is suggested to combine hypotheses testing with the serial bias compensation strategy for the bias detection [15].

The process starts from the null hypothesis, H_0, in which it is assumed there is no gross error and there is no bias adjustment for the measured data. The null hypothesis and the associated test statistics are given by:

$$
\begin{aligned}
&\boldsymbol{H_0}: \\
&\quad \textit{bias model}: \quad y'_j = f_j(a_i,\theta_k) + \varepsilon_j \\
&\quad \textit{test statistics}: \quad \chi^2_{H_0} = \sum_{j=1}^{m} \left(\frac{y'_j - f_j(a_i,\theta_k)}{\sigma_j} \right)^2
\end{aligned}
\tag{6}
$$

Without the hypothesized bias model, the test statistics for the null hypothesis is obtained from carrying out simultaneous data reconciliation and model calibration:

$$
\min_{a_i,\theta_k} \sum_{j=1}^{m} \left(\frac{y'_j - f_j(a_i,\theta_k)}{\sigma_j} \right)^2 \tag{7}
$$

When the test statistics rejects the null hypothesis, the hypotheses test on the gross error models, carried out by the serial bias compensation scheme, is then introduced. The serial bias compensation strategy can be performed in two ways as discussed in previous section. The first option is testing all possible bias models at different scenarios of total biases number. In the scenario of p biases, the alternative hypothesis for the qth bias model is given by [15]:

$$
\begin{aligned}
&H_1^{g_{pq}}: \\
&\quad \textit{bias model}: y'_j = f_j(a_i,\theta_k) + \varepsilon_j + (\boldsymbol{E}_{pq}\boldsymbol{b}_p)_j \\
&\quad \textit{test statistics}: \left.\chi^2_{H_1}\right)_{g_{pq}} = \sum_{j=1}^{m} \left(\frac{y'_j - (\boldsymbol{E}_{pq}\boldsymbol{b}_p)_j - f_j(a_i,\theta_k)}{\sigma_j} \right)^2
\end{aligned}
\tag{8}
$$

where $\boldsymbol{E}_{pq}$ represents the index matrix of the qth gross error model in the scenario of p biases. All elements except for the diagonal terms in the matrix $\boldsymbol{E}_{pq}$ are zero while number of p positions in the diagonal terms are equal to 1 and the rest diagonal elements are zeros. In each scenario of p biases, there are C_p^r bias models to be tested. Each bias model is simply represented by the index matrix $\boldsymbol{E}_{pq}$ with p non-zero elements in the diagonal terms. The structure of the index matrix $\boldsymbol{E}_{pq}$ is shown in Fig. 1. The test statistics for each bias hypothesis is obtained by carrying out the joint data reconciliation process given by [15]:

$$
\min_{a_i,\theta_k,b_p} \sum_{j=1}^{m} \left(\frac{y'_j - (\boldsymbol{E}_{pq}\boldsymbol{b}_p)_j - f_j(a_i,\theta_k)}{\sigma_j} \right)^2 \tag{9}
$$

where the magnitudes of the hypothesized biases, b_p, are optimized along with the model parameters, θ_k, and measurements, a_i.

The second option is eliminating gross error models one at a time. The alternative hypothesis for the mth gross error model at the lth round is given by:

$$
\begin{aligned}
&H_1^{g_{lm}/g_{l-1}/\ldots/g_1}: \\
&\quad \textit{bias model}: \quad y'_j = f_j(a_i,\theta_k) + \varepsilon_j + (\boldsymbol{E}_l\boldsymbol{b}_l)_j \\
&\quad \textit{test statistics}: \left.\chi^2_{H_1}\right)_{g_{lm}/g_{l-1}/\ldots/g_1} = \sum_{j=1}^{m} \left(\frac{y'_j - (\boldsymbol{E}_{lm}\boldsymbol{b}_l)_j - f_j(a_i,\theta_k)}{\sigma_j} \right)^2
\end{aligned}
\tag{10}
$$

where $\boldsymbol{E}_{lm}$ represents the index matrix of the m-th bias model at the l-th round hypotheses testing. Unlike $\boldsymbol{E}_{pq}$, there is only one floating element in the diagonal terms of $\boldsymbol{E}_{lm}$ at each round of hypotheses testing. In the l-th round of testing, there are (l – 1) non-zero elements at the fixed positions determined in the previous round, i.e., (l – 1)-th round. The number of all possible bias models at the l-th round is (r – l – 1) where r is the number of measured data. The structure of the index matrix $\boldsymbol{E}_{lm}$ is shown in Fig. 2.

Similarly, the test statistics for each bias hypothesis is obtained by carrying out the joint data reconciliation process, which is the least squares type minimization problem given by:

$$
\min_{a_i,\theta_k,b_l} \sum_{j=1}^{m} \left(\frac{y'_j - (\boldsymbol{E}_{lm}\boldsymbol{b}_l)_j - f_j(a_i,\theta_k)}{\sigma_j} \right)^2 \tag{11}
$$

where the magnitudes of the hypothesized biases, b_l, are optimized along with the model parameters, θ_k, and measurements, a_i.

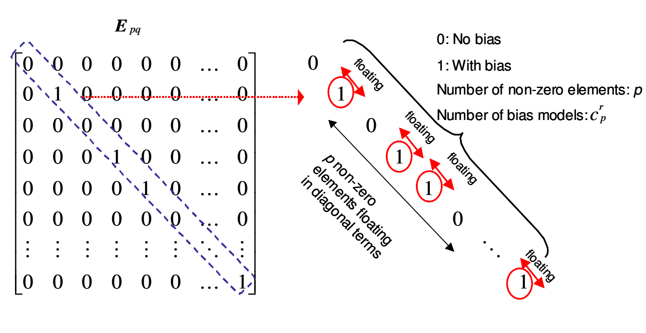

Figure 1 Structure of index matrix E_{pq}

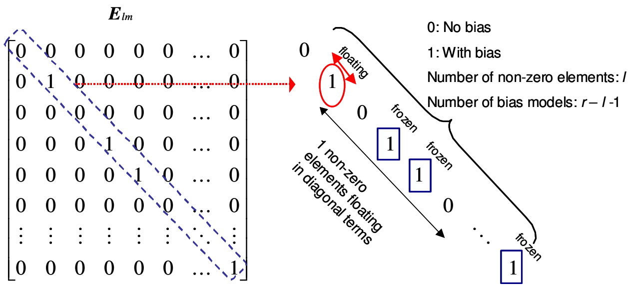

Figure 2 Structure of index matrix E_{lm}

In this study, the serial bias compensation was carried out within the MBDR scheme, which utilized the Lebenberg-Marquardt algorithm for solving the minimum Least Squares problem in different scenarios of bias models. RSE's were used to replace the GTP cycle model for the purpose of reducing computation time, especially in the bias detection process.

Data Filtering Using MSPCA

When processing the OSM data with MBDR, it is not practical to include all data sets due to increased computation time by adding more data. The use of filtering or denoising technique helps to screen large data sets down to manageable level. In this study, Multiscale Principal Component Analysis (MSPCA) is utilized to screen and select the data sets for the use in MBDR.

Multiscale Principal Component Analysis (MSPCA) [16-18] is widely used for data denoising in variety of fields. It combines the features of traditional Principal Component Analysis (PCA) [19] and Wavelets Transformation [20], making it best suited for analyzing the autocorrelated time-series signals like the plant performance data. In this study, MSPCA was used to filter the OSM data for the use of MBDR, serving as a systematic way of data selection from a large amount of sampled data.

Conventional PCA modeling is done at a single scale, where the model relates the data with the same time-frequency localization at all locations. For instance, PCA of a time series data is a single-scale model since it relates variables only at the scale of the sampling interval. The single-scale modeling is not appropriate most of the time since most data contains contributions at multiple scales.

On the other hand, the univariate wavelet analysis cannot catch the interrelations between different series of data that has multivariate nature embedded. Multiscale Principal Component Analysis (MSPCA) combines the multivariate feature of PCA with the multiscale characteristic of wavelet transformation. MSPCA extract the correlation among variables and combine it with orthonormal wavelets to separate deterministic features from the stochastic processes, while approximately decorrelate the autocorrelation among the measured variables.

The process of MSPCA is shown in Fig. 3. It starts from carrying out wavelet decomposition for each data series in the data matrix. Then the wavelet coefficients at each scale are grouped across series and PCA is performed at each scale. The wavelet coefficients at each scale are then reconstructed per retained PCA. Using T^2 and Q charts to create threshold, by which the wavelet coefficients are selected. Reconstruct all series only using scales that have points outside of threshold. Perform the final PCA for all scales together and reconstruct approximate data matrix from selected and thresholded wavelet coefficients.

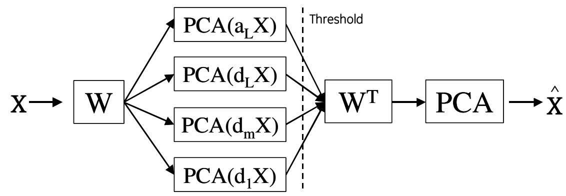

Figure 3 Methodology of MSPCA

The use of MSPCA requires that the multivariate data are linearly correlated. For the gas turbine performance data, the assumption of linear correlations is valid within a moderate change of ambient temperature and is based on the facts of chocked flow at stage 1 nozzle, regulated fuel by linear temperature control curve, and operation at a constant IGV and speed. By running the Monte Carlo Simulation of the GTP cycle deck over a 20°F change of temperature with the above conditions imposed, the scatter plot of multivariate gas turbine performance data, Fig. 4, shows the linear characteristics.

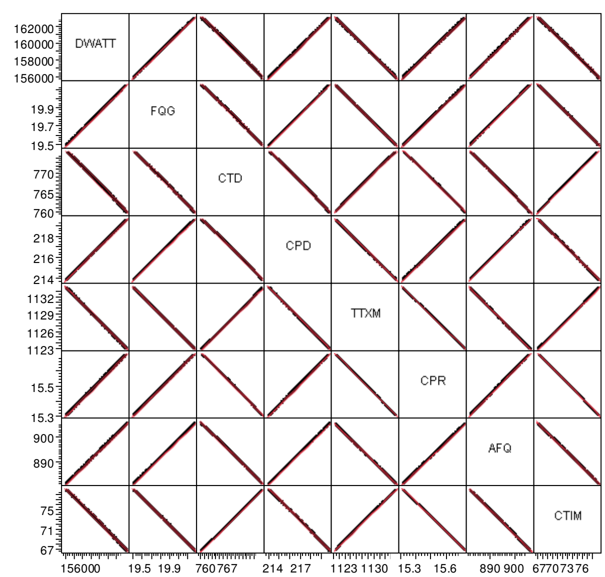

Figure 4 Scatterplot matrix of gas turbine performance characteristics

APPLICATION

A GE 7FA gas turbine was selected for the implementation of MBDR. The OSM data with 5-minute resolution was collected in a 24-hour sampling window, within which insignificant performance deterioration was assumed. The degradation status, as a result, can be represented by a set of model health parameters to be inferred by the sampled data. Only the steady-state-base-load data was considered. This is because the heat balance tools utilized in this study, GateCycle™ and GTP, are only valid for the steady-state simulation. The sampling window is adjustable depending on the degradation rate of the gas turbine unit. A preliminary investigation on the degradation rate is needed. It can be done by monitoring the changes of heath parameters over time calculated by traditional heat balance analysis on each data set, or by looking at the mean shifts of the pair-wise correlations between key parameters such as output versus ambient temperature. Sometimes the mean shifts are caused by changes of operation mode not by performance degradation, e.g., change of IGV, change from base load to peak load, etc. A careful look is needed to separate different causes.

Data Selection

In this study, only the measured data that serves as model outputs, e.g., DWATT, FQG, CTD, etc, are reconciled and used to infer the model calibration factors (or “health parameters”) such as DMM’s and Tfire. The operational parameters such as IGV, THN, FTG, etc, are typically controlled and maintained at certain target values with relatively small uncertainties. Instead of reconciling these operational parameters in the MBDR process, it is a reasonable way of simplification to propagate uncertainties of these parameters by correcting the measured model outputs. Uncertainties of the measured model outputs after corrections need to be reevaluated by combining uncertainties of those operational parameters used as correction references.

The measurements of ambient pressure and humidity usually have less uncertainty and are relatively stable compared to ambient temperature. Thus, these two parameters can also serve as correction parameters, and the corresponding uncertainties can be propagated to the measured model outputs using error propagation principle.

The corrected data were normalized by their means and standard deviations from the original raw data. In this study, the normalized data of ambient temperature and six corrected model outputs (Table 1) were selected for the MSPCA denoising process. The raw data were then compared against the denoised data and the data selection was carried out based on the Least Squares ranking for each data set. Either the raw data or de-noised data top ranked are selected and used for MBDR.

In the MSPCA analysis, the orthogonal wavelet bases used were the order 6 Symlet wavelets. The family of Symlet 6 has the characteristic of possessing the largest number of vanishing moments for a minimum support and hence was considered as the best choice in this study. This means, in the presence of gas turbine performance data at certain levels, the correlation between wavelet coefficients and the data would be high, yielding fewer and higher wavelet coefficient.

The level of wavelet decomposition should be selected to provide maximum separation between the stochastic and deterministic components of a time-series data. If the number of level is too small, a significant amount of noise will retain in the last scaled data resulted from MSPCA. A large number of decomposition levels could cause very few rows in the matrix of wavelet coefficient at coarser scales due to the dyadic downsampling, affecting the accuracy of PCA at that scale. The decomposition level can be decided by cross-validation, but in this study a heuristic maximum depth, $L = \log_2 n - 5$, was used, where n is the number of data set; L is the level of wavelet decomposition. The number of data sets was 142 in this studied example, and, therefore, the decomposition level, L, was 2. The Heuristic rule was used to determine the number of principal components retained at each decomposition level and at the final reconstruction step.

The MATLAB™ wavelet toolbox was utilized to perform MSPCA analysis. A 142 by 7 data matrix containing the normalized values for the corrected data of CTIM, DWATT, FQG, AFQ, TCD, PCD, and TTXM, was analyzed. The reconstructed time-series data of selected parameters are plotted against the original data shown in Fig. 5. The pairwise correlation plots of the denoised and raw data for the selected parameters are shown in and Fig. 6 and Fig. 7. As shown in these plots, the denoising effects are more obvious if the data are presented in a multivariate way, such as the pairwise correlation plot, than being presented in a univariate way, such as the time-series. This manifests the capability of MSPCA in ensuring mutual correlations among the denoised data that are more close to the physics-based model than the raw data. Figure 8, which zooms in one of the pairwise plot, DWATT vs. CTIM, demonstrates the denoised data represents the model behavior better than the raw data by tightening the DWATT/CTIM correlation.

The tightened correlation among performance parameters from the denoised data serves as a guideline of selecting the raw data used for MBDR, which is, selecting the raw data that are top ranked in least deviation from the corresponding denoised data. The data sets are ranked based on the Least Sqares scores, defined by the deviation between the raw and denoised data and the associated measurement uncertainty.

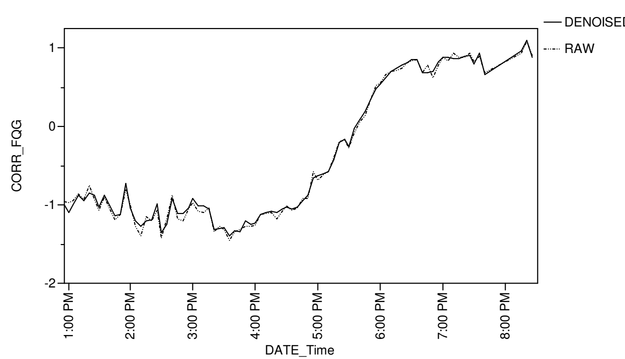

Figure 5 The denoised and raw data of corrected FQG

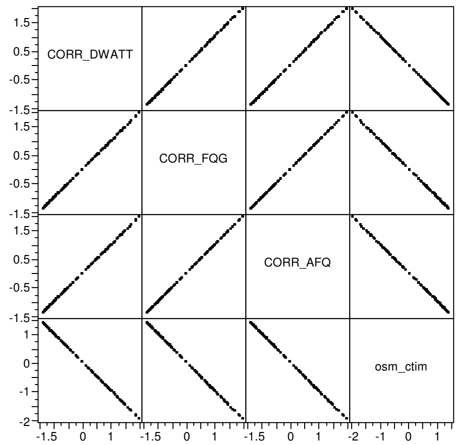

Figure 6 The pairwise correlation plot of the denoised data for the corrected DWATT, FQG, AFQ, and ambient temperature

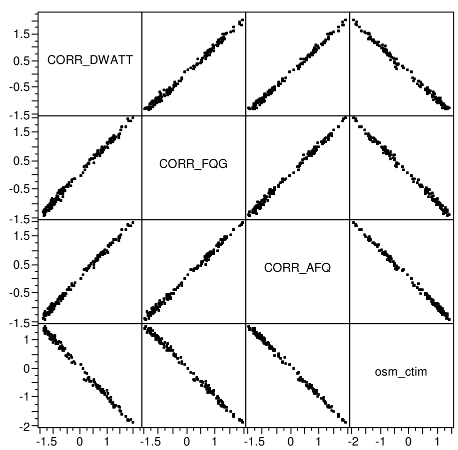

Figure 7 The pairwise correlation plot of the raw data for the corrected DWATT, FQG, AFQ, and ambient temperature

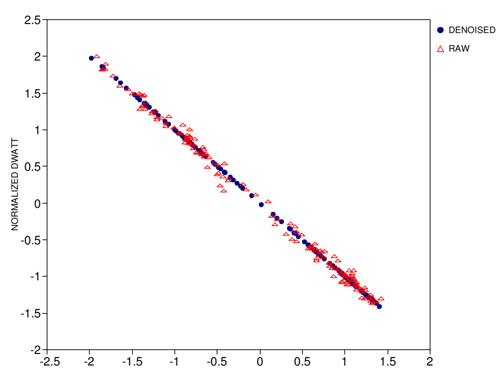

Figure 8 The correlation between normalized DWATT and ambient temperature

The Least Squares score for each data set can be calculated as follows:

$$S_i = \sum_{j=1}^{m} \left(\frac{y_j - \hat{y}_j}{\sigma_j} \right)^2 \qquad (12)$$

where S_i is the score of the *i*th data set; y_j , $\hat{y}_j$, and σ_j are the raw data, denoised data , and measurement uncertainty of the *j*th parameter. The 142 data sets were ranked based on their Least Squares scores from lowest to highest, and the top 10 data sets with the lowest scores were selected. It is also preferred to have a wide ambient range so we have higher confidence in utilizing the calibrated model for prediction across a wide ambient range. Therefore, both the Least Squares scores and ambient temperature range need to be considered when selecting the data sets.

MBDR and Bias Detection

The 10 data sets screened by MSPCA were used as the source data for MBDR. At each data set, the measured model outputs were corrected to the reference points of several ambient and operational parameters, assuming these correction parameters have less uncertainty and are relatively stable compared to others during the operation. The uncertainties of these corrected data were reevaluated by considering the uncertainties of the correction factors. The rest of measured model inputs, i.e., ambient temperature and pressure drops, served as constants in MBDR, i.e., no reconciliation for measured model inputs. The assumptions and simplifications were made for the purpose of reducing the computation time. In some special cases such as inlet bleed heating, the model input of ambient temperature will need to be reconciled due to non-uniform temperature profile. The MSPCA data screening process also helped to ensure the consistency between measured model inputs and outputs, but not able to differentiate data from biases.

For each data set, the response surface equations of gas turbine model outputs as functions of health parameters (DMM's and Tfire) were generated by the nonlinear regression utilizing the simulated data from Monte Carlo Simulation. A 2000-run Monte Carlo Simulation was carried out to generate random cases. The goodness-of-fit for each RSE was evaluated by examining the Reduced-Chi Squares, χ_v, and the residual plot, i.e., residuals should be normally distributed and pattern free for acceptance of goodness-of-fit. The RSE's were tested by comparisons with the GTP outputs through a 1000-run Monte Carlo Simulation. Table 2 summaries the averaged error of each simulated model output.

Table 2 The averaged error of RSE's compared to GTP model

DWATT	FQG	CDP	CTD	AFQ	TTXM
0.00253%	0.00028%	0.00020%	0.00013%	0.00021%	0.00133%

The RSE's were then used to replace the GTP model in MBDR. The reconciliation process can be expressed as follows:

$$\min_{\theta_i,\varphi_k} \sum_{k=1}^{5} \sum_{j=1}^{6} (y'_{jk} - f_{jk}(\theta_i, \varphi_k))^T \sigma_{jk}^{-1} (y'_{jk} - f_{jk}(\theta_i, \varphi_k)) \qquad (13)$$

where θ_i represent the cycle deck DMM's; φ_k is the firing temperature at the kth data set; y'_{jk} represents the measured data of the jth performance metric from the kth data set, while f_{jk} is the jth calculated performance metric at the corresponding operation condition of the kth data set.

Several scenarios of prior assumptions on the health parameters and measurement biases were tested. Currently the number of independent variables, i.e., health parameters, is equal to number of dependent variables, i.e., model outputs. This results in lack of information redundancy, which exists if the number of dependent variables is greater than number of independent variables. Prior knowledge or assumptions are, therefore, required by bias detection when information redundancy does not exist. Multiple data sets can only improve the location redundancy, i.e., a performance metric measured multiple times or having multiple measurement instruments. When systematic errors exist, location redundancy is not sufficient for detecting the biases, but information redundancy is. The information redundancy can be achieved through reducing the number of independent variables by introduction of prior knowledge or through increasing the number of performance characteristics being measured. The need for information redundancy is another reason why the measured model inputs were not suggested to be reconciled in MBDR.

No Bounds on Health Parameters. The first scenario is imposing no bounds on the health parameters including the firing temperature, and assuming there are no biases in measured model outputs. This allows MBDR to explore the design space for the health parameters as much as it can.

The Levenberr-Marquardt algorithm serves as a nonlinear solver to solve for Eq 1. The optimization process continues until the change of the chi-squares, $\Delta\chi^2$, i.e., the Least Squares objective function, is below $1*10^{-7}$ or the number of iterations exceeds 100. In this scenario, the converged Least Squares was 4.3, of which the Reduced-Chi-Squares was 0.095. The low Least Squares value indicates the average data adjustment is within the measurement uncertainty, ideal data reconciliation results. Table 3 shows the adjustments to measured model outputs in this scenario.

The means and standard deviations of the inferred health parameters are shown in Table 4. The results of the inferred health parameters showed the combustion efficiency DMM and the turbine CQ DMM exceeded the expected "new and clean" value, 1, significantly, suggesting there were serious heat imbalance and significant area growth in stage 1 nozzle area. It was shown, however, that the nozzle area input to the GTP cycle model in this study matched the test report issued recently, and, thus, it was less likely to have such a high turbine CQ DMM that indicates a big change in nozzle area. On the other hand, it is not possible to have combustion efficiency better than 100%. The DMM higher than 1 suggested there were significant heat imbalance, often caused by measurement biases in compressor airflow (AFQ) or fuel flow (FQG)

The prior knowledge about this unit can be utilized to constrain some health parameters, by which the degree of freedom in MBDR increases, i.e., information redundancy can exist. The bias detection scheme was then applied in the presence of information redundancy.

Bounds on Health Parameters. This scenario imposed bounds on two health parameters, combustion efficiency DMM and turbine CQ DMM, based on the facts that the combustion efficiency must not be greater than 1 and that the stage 1 nozzle area should not have such a big deviation from the test report. By bounding these two parameters to 1's, the degree of freedom was increased by two, allowing the bias detection scheme.

The sequential bias compensation was first applied. This scheme searches biases one at a time, while estimating the magnitudes of biases all together after previous biases are detected. Once it locates the first bias, searching on the second bias will be ran in the presence of first identified bias, and the magnitudes of both biases are estimated simultaneously. If all two-bias hypothesis models cannot lead to a better Least Squares, the scheme will end at the first identified bias.

The results from sequential bias detection are shown in Table 5 and 6. The AFQ bias was identified while no second bias was indicated. The RSE models were calibrated in the presence of the AFQ bias by MBDR where the health parameters along with the bias were solved all together for the minimum Least Squares. The estimated combustion efficiency DMM and turbine CQ DMM with AFQ bias identified are now close to 1's, and the estimated firing temperatures were about 13 °F higher than the nominal.

Table 3 Data adjustments for no bounds on health parameters

		Data 1	Data 2	Data 3	Data 4	Data 5	Data 6	Data 7	Data 8	Data 9	Data 10
DWATT	kW	56.81	67.81	-75.35	14.52	-6.90	-57.96	58.68	-45.50	-64.46	40.90
FQG	lb/sec	-0.02	-0.02	0.02	-0.01	0.01	0.01	-0.01	0.00	0.02	-0.02
CPD	psia	-0.12	-0.13	0.16	-0.04	0.03	0.07	-0.16	0.14	0.13	-0.07
CTD	F	-0.09	-0.03	-0.11	0.44	-0.05	0.24	0.45	-0.81	-0.04	0.03
AFQ	lb/sec	0.49	0.55	-0.92	0.33	0.27	-0.28	0.79	-0.44	-0.99	0.32
TTXM	F	-0.94	-1.28	1.33	-0.41	0.10	0.86	-1.52	1.29	1.09	-0.67

Table 4 Means and standard deviations of inferred health parameters in the scenario of no bounds on health parameters

	Mean	Std
comp_eff_DMM	0.9915	0.00078
comp_flow_DMM	1.0027	0.00152
comb_eff_DMM	1.0139	0.00246
turb_eff_DMM	0.9892	0.00081
turb_CQ_DMM	1.0327	0.00195
Tfire Data Set 1*	-4.7647	2.67384
Tfire Data Set 2	-4.9870	2.66911
Tfire Data Set 3	-5.3280	2.68816
Tfire Data Set 4	-4.7701	2.67655
Tfire Data Set 5	-5.9771	2.68282
Tfire Data Set 6	-5.0792	2.68560
Tfire Data Set 7	-4.6617	2.67085
Tfire Data Set 8	-4.8607	2.68708
Tfire Data Set 9	-5.1647	2.68884
Tfire Data Set 10	-3.6912	2.67193

Table 5 Data adjustments in the scenario of health parameters bounded

		Data 1	Data 2	Data 3	Data 4	Data 5	Data 6	Data 7	Data 8	Data 9	Data 10
DWATT	kW	32.14	19.37	-27.39	8.20	26.84	-18.55	12.22	-1.82	-14.03	-6.26
FQG	lb/sec	-0.03	-0.02	0.01	-0.02	-0.01	0.00	-0.01	-0.01	0.01	-0.02
CPD	psia	-0.13	-0.14	0.16	-0.05	0.03	0.07	-0.17	0.14	0.12	-0.09
CTD	F	-0.09	-0.03	-0.12	0.43	-0.06	0.23	0.46	-0.83	-0.06	0.03
AFQ	lb/sec	-24.15	-23.97	-26.08	-24.42	-24.77	-25.37	-23.74	-25.56	-26.18	-24.19
TTXM	F	-0.49	-0.50	0.86	-0.21	-0.21	0.48	-0.77	0.87	0.58	0.11

Table 6 Estimated health parameters and the measurement bias in the scenario of health parameters bounded

	Mean	Std
comp_eff_DMM	0.9915	0.00078
comp_flow_DMM	0.9757	0.00152
comb_eff_DMM	0.9960	0.00243
turb_eff_DMM	1.0004	0.00089
turb_CQ_DMM	1.0011	0.00191
Tfire Data Set 1*	13.7341	2.71227
Tfire Data Set 2	13.7004	2.70871
Tfire Data Set 3	12.7534	2.72359
Tfire Data Set 4	13.6000	2.71506
Tfire Data Set 5	12.1519	2.71983
Tfire Data Set 6	13.0367	2.72261
Tfire Data Set 7	14.0095	2.70960
Tfire Data Set 8	13.2387	2.72418
Tfire Data Set 9	12.9013	2.72370
Tfire Data Set 10	15.0064	2.70989

Biases	Unit	Biase (sigma)
DWATT	Sigma	0
FQG	Sigma	0
CPD	Sigma	0
CTD	Sigma	0
AFQ	Sigma	-5.63
TTXM	Sigma	0

The alternative option of hypothesis test is testing all possible bias models. If the MBDR has *n* degree of freedom, the bias detection scheme is good for identifying up to *n* biases, while multiple solutions might exist. If one is trying to detect more biases, more constraints from prior assumptions or engineering judgments are required for decision making among multiple solutions. The test scenarios will include number of C_1^6 tests on the one-bias scenario, number of C_2^6 tests on the two-bias scenario, etc, and up to number of C_n^6 tests on the *n*-bias scenario. In this case with two degree of freedom available, the bias detection is required to test total number of $C_1^6 + C_2^6 = 21$ bias models. Table 7 lists the test results for all of the 1-bias and 2-bias scenarios. The results show that, in the 1-bias scenario, the model of AFQ bias with –5.63 standard deviation correction has the best Least Squares score while the corresponding estimates of model health parameters were within expectations. The fact that the reading of AFQ (compressor airflow) often had bias due to miscalculation suggested this AFQ bias model was acceptable. The second ranked model of CDP bias suggested a large correction of CDP while resulting in comb_eff_DMM greater than 1, which was not accepted by the engineering expectation. For the 2-bias scenario, the top 2 ranked bias models that had better Least Squares scores than the best 1-bais model both suggested the AFQ bias. The first bias model also suggested a FQG bias, but the estimated magnitude was within its measurement uncertainty. The second model suggested a TTXM bias of 2-standard-deviation magnitude, not categorized as a bias. This explained the reason of not identifying the 2-bias model by the algorithm of sequential bias compensation.

Table 7 Hypothesis testing results for all 1-bias and 2-bias scenarios with the estimated firing temperatures of the first 5 datasets

	Least Squares	DWATT	FQG	CDP	CDT	AFQ	TTXM	comp_eff_DMM	comp_flow_DMM	comb_eff_DMM	turb_eff_DMM	turb_CQ_DMM	Tfire Data Set 1*	Tfire Data Set 2	Tfire Data Set 3	Tfire Data Set 4	Tfire Data Set 5
1 bias	**1.05250**					**-5.63**		**0.9915**	**0.9756**	**0.9960**	**1.0004**	**1.0011**	**13.7**	**13.7**	**12.8**	**13.6**	**12.2**
	1.67685			14.05				1.0037	1.0025	1.0116	0.9839	0.9997	-1.0	-1.2	-2.0	-1.1	-2.5
	4.22514	-25.64						0.9919	0.9996	0.9901	0.9707	1.0226	-34.3	-34.4	-35.6	-34.5	-36.0
	4.24748						-10.12	0.9919	0.9996	0.9915	1.0035	1.0229	-32.4	-32.6	-33.1	-32.4	-33.8
	5.06700				-23.66			1.0500	0.9991	1.0097	0.9704	1.0192	-31.0	-31.2	-31.4	-31.0	-32.1
	6.37885		1.48					0.9920	0.9984	1.0010	0.9906	1.0268	-3.1	-3.3	-3.7	-3.1	-4.3
2 biases	0.98029		-0.92			-6.05		0.9915	0.9736	1.0000	1.0015	0.9987	15.6	15.6	14.6	15.5	14.0
	1.02416					-5.85	1.56	0.9915	0.9746	0.9982	0.9988	1.0007	19.0	18.9	18.0	18.9	17.4
	1.06362			3.96		-4.26		0.9950	0.9823	0.9999	0.9960	0.9998	10.1	10.0	9.2	10.0	8.6
	1.20271	4.40				-5.91		0.9915	0.9743	0.9986	1.0044	1.0005	20.0	20.0	19.3	20.0	18.6
	1.20496			12.93			-5.97	1.0028	1.0030	1.0009	0.9918	0.9999	-19.0	-19.1	-19.9	-19.1	-20.5
	1.23934		2.14	14.64				1.0042	1.0032	0.9999	0.9831	0.9995	-2.2	-2.3	-3.1	-2.2	-3.7
	1.29510				5.03	-5.80		0.9800	0.9749	0.9955	1.0050	1.0019	20.0	20.0	19.2	20.0	18.6
	1.72883			13.47	-0.02			1.0033	1.0023	1.0115	0.9842	1.0009	-1.1	-1.3	-2.0	-1.2	-2.6
	2.02299	2.90		13.43				1.0031	1.0019	1.0136	0.9866	1.0011	2.7	2.5	1.9	2.6	1.3
	4.26300	10.55					-14.21	0.9919	0.9995	0.9922	1.0171	1.0230	-31.4	-31.6	-31.8	-31.4	-32.6
	4.26748				-8.75		-9.18	1.0125	0.9997	0.9933	0.9948	1.0204	-40.0	-40.0	-40.0	-40.0	-40.0
	4.61248	-30.69	-2.66					0.9918	0.9991	1.0011	0.9673	1.0207	-39.0	-39.0	-40.0	-39.2	-40.0
	4.92974		-2.92				-13.34	0.9917	0.9990	1.0021	1.0085	1.0203	-39.9	-40.0	-40.0	-40.0	-40.0
	5.09460	-18.49			-12.62			1.0220	0.9996	0.9958	0.9653	1.0196	-40.0	-40.0	-40.0	-40.0	-40.0
	6.38885		1.45		-1.07			0.9944	0.9983	1.0011	0.9898	1.0264	-4.2	-4.4	-4.8	-4.2	-5.5

*Delta firing temperature, difference between estimated and nominal

The uncertainties of inferred model health parameters by MBDR were also evaluated and compared to the traditional data reduction method. Figure 9 shows the normal distributions of the estimated compressor efficiency DMM's (comp_eff_DMM) by MBDR and tradition data reduction method.

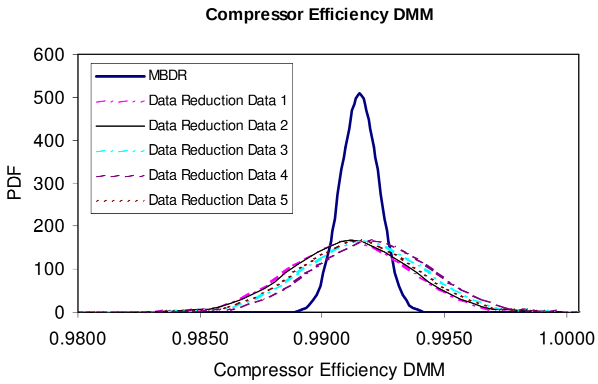

Figure 9 Uncertainty of compressor efficiency DMM

Figure 9 shows that the uncertainty of compressor efficiency DMM was reduced significantly due to the use of multiple data sets. It is also shown that MBDR leads to a single estimated value for the model health parameters (except for firing temperature) instead of different values at different data sets. The features of unified estimates with reduced uncertainty are especially desired in reducing the risk of performance prediction and guarantee.

CONCLUSION

A methodology of model-based data reconciliation (MBDR) and bias detection has been developed for solving the problem of gas turbine model calibration using the OSM data, which are subjected to larger measurement uncertainty and biases. A method of data filtering and selection using MSPCA is proposed. This scheme can be utilized to filter large amount of OSM data while ensuring the filtered/selected data still satisfy the linear correlations between performance characteristics in gas turbine. Within a moderate range of ambient temperature, the linear correlations can be achieved by correcting out the ambient pressure and humidity effects.

Multiple data sets, selected by MSPCA, are used as source data for MBDR. The use of multiple data sets reduces the uncertainty of model turners, i.e., health parameters, and, therefore, improves the quality of calibrated model. The RSE's serve as surrogate models to reduce the computation time. The time saving is especially prominent when the bias detection scheme is executed. The method of sequential bias compensation has shown its capability of detecting biases. It needs less execution of MBDR than the scheme of hypothesis testing on all bias models. Future works will focus on testing the bias detection scheme in more gas turbine units and improving its detection rate.

REFERENCES

[1] Romagnoli, J. A., Sanchez, M. C., 2000, Data Processing and Reconciliation for Chemical Process Operations: Volume Two (Process System Engineering, 1st Ed., Academic Press, New York.
[2] Crowe C. M., Y. A. G. Campos and A. Hrymak, Reconciliation of process flow rates by matrix projection. Part I: linear case. AIChE Jl 29, 881 (1983).
[3] Pai C. C. D. and G. D. Fisher, Application of Broyden's method to reconciliation of nonlinearly constrained data. AIChE Jl 34, 873 (1988).
[4] Swartz C. L. E., Data reconciliation for generalized flow-sheet applications. Paper presented at American Chem Soc. National Mtg, Dallas, TX (1989).
[5] Tjoa I. B. and L. T. Biegler, Simultaneous solution and optimization strategies for parameter estimation of differential-algebraic equation systems. Ind. Engng Chem. Res. 30, 376 (1991)
[6] Tamhane A. C. and R. H. S. Mah, Data reconciliation and gross error detection in chemical process networks. Technometrics 27, 409 (1985).
[7] Rosenberg J., R. S. H. Mah and C. Jordache, Evaluation of schemes for detecting and identifying gross errors in process data. Ind. Engng. Chem. Res. 26, 555 (1987).
[8] Narasimhan S. and R. H. S. Mah, Treatment of general steady state process models in gross error identification. Computers chem.. Engng 13, 851 (1989)
[9] Cheng, P. C., Andersen, H., The Implementation of the Data Validation Process in a Gas Turbine Performance Monitoring System, ASME Paper GT-2005-68429 (2005).
[10] Harter, P., J. Petek, and P. Pechtl, Model-Based Data Reconciliation to Improve Accuracy and Reliability of Performance Evaluation of Thermal Power Plants, ASME Paper GT2005-68937 (2005).
[11] Gulen, S. C., and R. W. Smith, A Simple Mathematical Approach to Data Reconciliation in a Single-Shaft Combined-Cycle System, ASME Paper GT2006-90145, 2006.
[12] Doel D.L., 1992, 'Temper - a Gas Path Analysis tool for commercial jet engines', 92-GT-315.
[13] Urban L.A., 1972, 'Gas Path analysis applied to turbine engine condition monitoring', AIAA 72-1082.
[14] Kamboukos Ph., Mathioudakis K., 2003, 'Comparison of linear and non-linear gas turbine performance diagnostics', ASME GT-2003-38518.
[15] Lin, TsungPo, 2008. "An Adaptive Modeling and Simulation Environment for Combined-Cycle Data Reconciliation and Degradation Estimation ". PhD Thesis, Georgia Institute of Technology, Atlanta GA
[16] M. Lampton. "Damping-Undamping Strategies for the Levenberg-Marquardt Nonlinear Least-Squares Method," Computers in Physics Journal, 11(1): 110-115, Jan./Feb. 1997
[17] Aminghafari, M.; Cheze, N.; Poggi, J-M. (2006), "Multivariate de-noising using wavelets and principal component analysis," Computational Statistics & Data Analysis, 50, pp. 2381–2398.
[18] Bakshi, B. (1998), "Multiscale PCA with application to MSPC monitoring," AIChE J., 44, pp. 1596–1610.
[19] Hotelling H., "Analysis of a Complex of Statistical Variables into Principal Components". Journal of Educational Psychology, 24:417–441, 1933
[20] Mallat, S. (1989), "A theory for multiresolution signal decomposition: the wavelet representation," IEEE Pattern Anal. and Machine Intell., vol. 11, no. 7, pp. 674–693.

